trans-[Ni(333-tet)(μ-N_3)]$_n$(ClO_4)$_n$ and *cis*-[Ni(333-tet)(μ-N_3)]$_n$(PF_6)$_n$: Two Novel Kinds of Structural Nickel(II) Chains with a Single Azido Bridge. Magnetic Behavior of an Alternating S = 1 chain with α = 0.46

Albert Escuer,*,† Ramon Vicente,† Joan Ribas,† M. Salah El Fallah,† Xavier Solans,‡ and Mercé Font-Bardía‡

Departament de Química Inorgànica, Universitat de Barcelona, Diagonal 647, 08028-Barcelona, Spain, and Departament de Cristal.lografia i Mineralogia, Universitat de Barcelona, Martí Franqués s/n, 08028-Barcelona, Spain

Received September 17, 1993®

The compounds *trans*-[Ni(333-tet)(μ-N_3)]$_n$(ClO_4)$_n$ (**1**) and *cis*-[Ni(333-tet)(μ-N_3)]$_n$(PF_6)$_n$ (**2**) in which 333-tet is the tetraamine *N,N'*-bis(3-aminopropyl)-1,3-propanediamine have been synthesized and characterized. **1** crystallizes in the triclinic system, space group $P\bar{1}$, with fw = 388.50, a = 8.765(1) Å, b = 8.976(1) Å, c = 11.995(2) Å, α = 106.65(1)°, β = 110.06(1)°, γ = 91.11(1)°, V = 842.0(2) Å^3, Z = 2, R = 0.047, and R_w = 0.130. The nickel atom is placed in an octahedral environment with the bridging azido groups in a *trans* arrangement. Two kinds of alternating centrosymmetric azido bridges, both coordinated in end-to-end fashion, are present in the chain, for which the Ni–N bond distance and Ni–N–N bond angle are 2.077(3) Å, 142.4(3)° and 2.204(3) Å, 123.6(2)°, respectively, giving an unusual alternating system. **2** crystallizes in the orthorhombic system, space group $P2_12_12_1$, with fw = 434.03, a = 15.736(3) Å, b = 13.607(3) Å, c = 8.182(2) Å, V = 1751.9(7) Å^3, Z = 4, R = 0.062, and R_w = 0.154. The nickel atom is placed in an octahedral environment with the end-to-end azido bridges in an unprecedented *cis* arrangement. Magnetic measurements show a strong antiferromagnetic coupling for **1**, where J = −80.7 cm^{-1}, α = 0.46, and g = 2.40, and lower coupling for **2**, where J = −18.5 cm^{-1} and g = 2.29. The magnetic behavior of both compounds has been correlated with the bond parameters.

Introduction

In the past two decades the azido ligand has been investigated as a very efficient superexchange pathway between paramagnetic ions such as copper,[1-5] nickel,[6-14] cobalt,[15] manganese,[16,17] or chromium.[18] For all of them it is well established that end-to-end coordination (EE) gives antiferromagnetic systems, whereas when the coordination is end-on (EO) ferromagnetic systems are obtained. The most common kind of compound is the dinuclear one, in which both EE and EO compounds show double azido bridge and *cis* coordination. Recently we have reported the synthesis of several monodimensional nickel(II) compounds bridged by the azido ligand: [Ni_2(dpt)$_2$(μ-N_3)$_3$]$_n$(ClO_4)$_n$, in which dpt is bis(3-aminopropyl)amine, a structural and magnetic alternating (–(N_3)–NiL–(N_3)$_2$–NiL–)$_n$ chain,[19] and a series of monobridged EE azido 1D systems tailored from *trans* tetraamine complexes of nickel(II), with a generic formula *trans*-[Ni(L)(μ-N_3)]$_n$(ClO_4)$_n$, in which L = cyclam[20] (1,4,8,11-tetraazacyclotetradecane), 232-tet[21] (*N,N'*-bis(2-aminoethyl)-1,3-propanediamine), 323-tet[21] (*N,N'*-bis(3-aminopropyl)-1,2-ethanediamine), *m*-CTH[22] (*meso*-5,7,7,12,14,14-hexamethyl-1,4,8,11-tetraazacyclotetradecane), or M5[22] (2,3-dimethyl-1,4,8,11-tetraazacyclotetradeca-1,3-diene). The first four *trans*-[Ni(L)(μ-N_3)]$_n$(ClO_4)$_n$ compounds are uniform (–(N_3)–NiL–(N_3)–NiL–)$_n$ chains, and the last is an alternating system; according to the general trends indicated above all five compounds show an antiferromagnetic behavior. J values have been correlated with structural parameters (mainly bond angles) in a very recent work.[21] Following this synthetic pathway, we present now two new 1D compounds in which L is the tetraamine 333-tet (*N,N'*-bis(3-aminopropyl)-1,3-propanediamine): *trans*-[Ni(333-tet)(μ-N_3)]$_n$(ClO_4)$_n$ (**1**) and *cis*-[Ni(333-tet)(μ-N_3)]$_n$(PF_6)$_n$ (**2**). Compound **1** presents the azido groups coordinated in end-to-end fashion in *trans* arrangement around the nickel atom, but the structural data indicate the presence along the chain axis of the unusual (–NiL–(N_3)–NiL–(N_3)'–)$_n$ scheme, in which the azido

† Departament de Química Inorgànica.
‡ Departament de Cristallographia i Mineralogia.
® Abstract published in *Advance ACS Abstracts,* March 15, 1994.

(1) Felthouse, T. R.; Hendrickson, D. N. *Inorg. Chem.* **1978**, *17*, 444.
(2) Comarmond, J.; Plumeré, P.; Lehn, J. M.; Agnus, Y.; Louis, R.; Weiss, R.; Kahn, O.; Morgensten-Badarau, I. *J. Am. Chem. Soc.* **1982**, *104*, 6330.
(3) Boillot, M. L.; Journaux, Y.; Bencini, A.; Gatteschi, D.; Kahn, O. *Inorg. Chem.* **1985**, *24*, 263.
(4) Charlot, M. F.; Kahn, O.; Chaillet, M.; Larrieu, C. *J. Am. Chem. Soc.* **1986**, *108*, 2574.
(5) Chaudhuri, P.; Oder, K.; Wieghardt, K.; Nuber, B.; Weiss, J. *Inorg. Chem.* **1986**, *25*, 2818.
(6) Wagner, F.; Mocella, M. T.; D'Aniello, M. J.; Wang, A. H. J.; Barefield, E. K. *J. Am. Chem. Soc.* **1974**, *96*, 2625.
(7) Pierpont, C. G.; Hendrickson, D. N.; Duggan, D. M.; Wagner, F.; Barefield, E. K. *Inorg. Chem.* **1975**, *14*, 604.
(8) Chaudhuri, P.; Guttmann, M.; Ventur, D.; Wieghardt, K.; Nuber, B.; Weiss, J. *Chem. Commun.* **1985**, 1618.
(9) Arriortua, M. I.; Cortes, A. R.; Lezama, L.; Rojo, T.; Solans, X.; Font-Bardia, M. *Inorg. Chim. Acta* **1990**, *174*, 263.
(10) Escuer, A.; Vicente, R.; Ribas, J. *J. Magn. Magn. Mater.* **1992**, *110*, 181.
(11) Cortes, A. R.; Ruiz de Larramendi, J. I.; Lezama, L.; Rojo, T.; Urtiaga, K.; Arriortua, M. I. *J. Chem. Soc., Dalton Trans.* **1992**, 2723.
(12) Ribas, J.; Monfort, M.; Costa, R.; Solans, X. *Inorg. Chem.* **1993**, *32*, 695.
(13) Vicente, R.; Escuer, A.; Ribas, J.; El Fallah, M. S.; Solans, X.; Font-Bardia, M. *Inorg. Chem.* **1993**, *32*, 1920.
(14) Ribas, J.; Monfort, M.; Diaz, C.; Bastos, C.; Solans, X. *Inorg. Chem.* **1993**, *32*, 3557.
(15) Bencini, A.; Ghilardo, C. A.; Midollini, S.; Orlandini, A. *Inorg. Chem.* **1989**, *28*, 1958.
(16) Stults, B. R.; Marianelli, R. S.; Day, V. W. *Inorg. Chem.* **1975**, *14*, 722.
(17) Goher, M. A. S.; Abu-Youssef, M. A. M.; Mautner, F. A.; Popitsch, A. *Polyhedron* **1992**, *11*, 2137.
(18) Goher, M. A. S.; Abu-Youssef, M. A. M.; Mautner, F. A. *Z. Naturforsch.* **1992**, *47b*, 139.
(19) Vicente, R.; Escuer, A.; Ribas, J.; Solans, X. *Inorg. Chem.* **1992**, *31*, 1726.
(20) Escuer, A.; Vicente, R.; Ribas, J.; El Fallah, M. S.; Solans, X. *Inorg. Chem.* **1993**, *32*, 1033.
(21) Escuer, A.; Vicente, R.; Ribas, J.; El Fallah, M. S.; Solans, X.; Font-Bardia, M. *Inorg. Chem.* **1993**, *32*, 3727.
(22) Escuer, A.; Vicente, R.; El Fallah, M. S.; Ribas, J.; Solans, X.; Font-Bardia, M. *J. Chem. Soc., Dalton Trans.* **1993**, 2975.

0020-1669/94/1333-1842$04.50/0

ligand is bonded with two distinctly different sets of bond distances and angles, giving a new first example of a monobridged μ-azido structurally alternating chain. Compound **2** is a uniform $(-(N_3)-NiL-(N_3)-NiL-)_n$ system but, surprisingly, shows the unprecedented *cis* coordination, giving the first case[23] in which *cis* arrangement does not correspond to a dinuclear compound. Both compounds are antiferromagnetically coupled in agreement with the EE mode of coordination of the azido bridge.

The alternation in the Ni–N(azido) distances and angles in compound **1** implies an alternation in the J coupling constant, and this chain should be analyzed by a theoretical model which takes into account the alternation in magnetic interactions along the chain. Experimentally, this kind of alternating system has only been studied for $S = {}^1/_2$ Heisenberg chains,[24] using the Hamiltonian $H = -2J\Sigma_i[S_{i-1}\cdot S_i + \alpha S_i\cdot S_{i+1}]$, where the alternating chain is defined for $0 < \alpha < 1$. For $\alpha = 0$ a dimeric behavior is obtained, and for $\alpha = 1$ the magnetic behavior corresponds to a uniform chain, for which χ_M tends to a finite value at low temperature. To our knowledge, only one $S = 1$ alternating 1D system (oxo-bridged iron(IV)) has been studied and reported to date.[25]

In this study, we present the structural and magnetic characterization of compounds **1** and **2** and we develop the correlation between their magnetic properties with the angle-dependent model proposed in the previous paper.[21]

Experimental Section

Synthesis. Caution! Perchlorate salts of metal complexes with azide and organic ligands are potentially explosive. Only a small amount of material should be prepared, and it should be handled with caution.

Compound **1** was obtained by starting with a solution of 2 mmol of nickel(II) perchlorate hexahydrate in 30 mL of water mixed with 2 mmol of 333-tet ligand. After 5 min of stirring, the resulting solution was mixed with 2 mmol of sodium azide dissolved in 10 mL of water. Compound **2** was obtained by using the same method as for **1**, starting from nickel(II) nitrate hexahydrate and 2.5 mmol of potassium hexafluorophosphate.

Slow evaporation of the resulting blue solutions gave dark blue crystals of the corresponding 1D compound, yield >80%. Both complexes are very soluble in water and slightly soluble in the common organic solvents. Elemental analyses of C, H, and N (Cl for **1**) are in good agreement with the title compounds.

Synthesis of *trans* and *cis* isomers of $[Ni(333\text{-tet})]^{2+}$ cannot be considered surprising taking into account that for this kind of tetraaminate ligand an equilibrium between the two conformations occurs in aqueous medium. Generally, the trans arrangement is preferred, but solvent effects in solution or the solubility effect due to the counteranion in solid state[26] can stabilize a specific conformation. Even with the same counteranion, for the 232-tet ligand, we have obtained simultaneously the dinuclear compound *cis*-$(\mu\text{-}N_3)_2[Ni(232\text{-tet})]_2(ClO_4)_2$[13] and the 1D one *trans*-$[Ni(232\text{-tet})(\mu\text{-}N_3)]_n(ClO_4)_n$.[21]

IR and Magnetic Measurements. IR spectra were recorded on a Nicolet 520 FTIR spectrophotometer. Magnetic measurements were carried out on polycrystalline samples with a pendulum type magnetometer (Manics DSM8) equipped with a helium continuous-flow cryostat working in the 300–4 K range and a Drusch EAF 16UE electromagnet. The magnetic field was approximately 15 000 G. Diamagnetic corrections were estimated from the Pascal tables.

X-ray Crystallography. Similar prismatic blue crystals (0.1 mm × 0.1 mm × 0.2 mm) were selected and mounted on an Enraf-Nonius CAD4 for **1** and a Philips PW-1100 diffractometer for **2**. Unit cell parameters were determined from automatic centering of 25 reflections $12 \le \theta \le 16°$ for **1** and $8 \le \theta \le 16°$ for **2** and refined by least-squares methods. Intensities were collected with graphite-monochromatized Mo Kα radiation, using the $\omega/2\theta$ scan technique. Three reflections were measured every 2 h as orientation and intensity controls; significant intensity decay was not observed. Lorentz-polarization and extinction, (coefficients 0.022(4) for **1** and 0.009(3) for **2**), but not absorption, corrections were made. The crystallographic data, conditions used for the intensity data collection, and some features of the structure refinement for both compounds are listed in Table 1. The structures were solved by Patterson synthesis, using the SHELXS computer program,[27] and refined by full-matrix least-squares methods, with the SHELX93 computer program.[28] The functions minimized were $\Sigma w||F_o| - |F_c||^2$, where $w = (\sigma^2(F_o) + 0.0052|F_o|^2)^{-1}$, for **1** and $\Sigma\sigma^2|F_o^2| + (0.1254P)^2 + 2.1781P$, where $P = (F_o^2 + 2F_c^2)/3$, for **2**. f, f', and f'' values were taken from ref 29. All hydrogen atom positions were determined from a difference synthesis, which was refined with an overall isotropic temperature factor (using a riding model for **2**). For compound **2**, fluorine atoms of the hexafluorophosphate ion were located in disordered positions; the occupancy factor was refined, with final values 0.51(2) and 0.49(2), and all F atoms were refined isotropically. The number of parameters refined for **1** was 276 and for **2** was 214. A test of chirality was performed for **2**, with Flack parameter –0.04(7). Final atomic coordinates are given in Table 2 for **1** and Table 3 for **2**.

Table 1. Crystal Data for *trans*-$[Ni(333\text{-tet})(\mu\text{-}N_3)]_n(ClO_4)_n$ (**1**) and *cis*-$[Ni(333\text{-tet})(\mu\text{-}N_3)]_n(PF_6)_n$ (**2**)

	1	**2**
chem formula	$[C_9H_{24}N_7Ni]_n(ClO_4)_n$	$[C_9H_{24}N_7Ni]_n(PF_6)_n$
a, Å	8.765(1)	15.736(3)
b, Å	8.976(1)	13.607(3)
c, Å	11.995(2)	8.182(2)
α, deg	106.65(1)	90.0
β, deg	110.06(1)	90.0
τ, deg	91.11(1)	90.0
V, Å^3	842.0(2)	1751.9(7)
Z	2	4
fw	388.50	434.03
space group	$P\bar{1}$	$P2_12_12_1$
T, °C	25	25
λ(Mo Kα), Å	0.710 69	0.710 69
d_{calc}, g/cm^3	1.532	1.646
μ(Mo Kα), cm^{-1}	13.37	12.70
$R(F_o)^a$	0.047	0.062
$R_w(F_o)^b$	0.130	0.154

^{a} $R(F_o) = \Sigma w||F_o| - |F_c||/\Sigma w|F_o|$. ^{b} $R_w(F_o) = \Sigma w||F_o|^2 - |F_c|^2|/\Sigma w|F_o|^2$.

Table 2. Positional Parameters and Equivalent Isotropic Displacement Parameters (Å^2 × 10^3) and Their Estimated Standard Deviations for *trans*-$[Ni(333\text{-tet})(\mu\text{-}N_3)]_n(ClO_4)_n$ (**1**)

atom	x/a	y/b	z/c	U_{eq}
Ni	1.0545(1)	1.0159(1)	0.2697(1)	34(1)
N(1)	1.1099(4)	1.2599(3)	0.3647(3)	50(1)
N(2)	1.3128(3)	0.9984(4)	0.3269(3)	51(1)
N(3)	0.9704(3)	0.7694(3)	0.1808(3)	46(1)
N(4)	0.8065(4)	1.0449(4)	0.2443(3)	56(1)
N(5)	1.0455(6)	1.0572(5)	0.1059(3)	86(1)
N(6)	1.0000	1.0000	0.0000	43(1)
N(7)	1.0922(3)	0.9755(4)	0.4495(3)	50(1)
N(8)	1.0000	1.0000	0.5000	37(1)
C(1)	1.2458(6)	1.3508(4)	0.3586(4)	67(1)
C(2)	1.4065(5)	1.2893(5)	0.4113(5)	74(1)
C(3)	1.4218(5)	1.1309(5)	0.3328(5)	74(1)
C(4)	1.3619(5)	0.8501(5)	0.2680(5)	71(1)
C(5)	1.2594(6)	0.7047(5)	0.2592(5)	74(1)
C(6)	1.0913(6)	0.6662(4)	0.1545(5)	69(1)
C(7)	0.8155(5)	0.7237(5)	0.0678(4)	63(1)
C(8)	0.6673(5)	0.7923(6)	0.0872(4)	70(1)
C(9)	0.6791(5)	0.9669(6)	0.1192(4)	63(1)
Cl	0.7294(1)	1.4801(1)	0.2799(1)	58(1)
O(1)	0.7672(5)	1.3965(4)	0.3706(4)	89(1)
O(2)	0.7966(8)	1.6387(5)	0.3406(4)	141(2)
O(3)	0.7975(7)	1.4112(6)	0.1907(5)	125(2)
O(4)	0.5607(5)	1.4678(7)	0.2204(6)	138(2)

(23) During the preparation of this manuscript, a second *cis-catena* complex of nickel(II), using bipy as a blocking ligand, has been characterized: Cortés, R., Universidad del Pais Vasco, Bilbao, Spain. Private communication.
(24) Carlin, R. L. *Magnetochemistry*; Springer Verlag: Berlin, 1986; pp 184–186.
(25) Hiller, W.; Strähle, J.; Datz, A.; Hanack, M.; Hatfield, W. E.; Haar, L. W.; Gütlic, P. *J. Am. Chem. Soc.* **1984**, *106*, 329.
(26) Cook, D. F.; McKenzie, E. D. *Inorg. Chim. Acta* **1978**, *31*, 59.
(27) Sheldrick, G. M. *Acta Crystallogr.* **1990**, *A46*, 467.
(28) Sheldrick, G. M.; *J. Appl. Crystallogr.*, in press.
(29) *International Tables for X-ray Crystallography*; Kynoch Press: Birmingham, England, 1974; Vol. IV, pp 99–110 and 149.

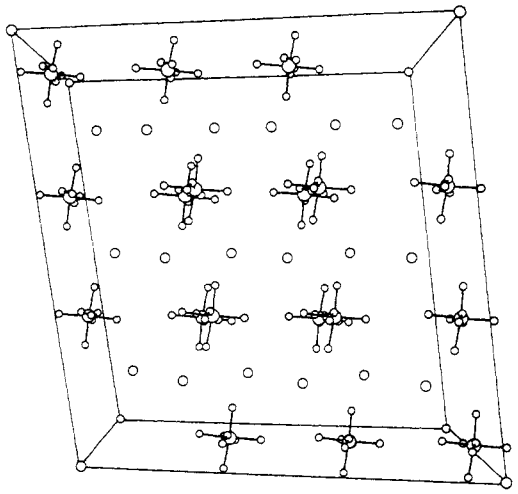

Figure 1. Axial view of four unit cells of compound **1**, showing the packing of the chains. Only nickel, nitrogen, and chlorine atoms are shown for clarity.

Table 3. Positional Parameters and Equivalent Isotropic Displacement Parameters ($Å^2 \times 10^3$) and Their Estimated Standard Deviations for *cis*-$[Ni(333\text{-tet})(\mu\text{-}N_3)]_n(PF_6)_n$ (**2**)

atom	x/a	y/b	z/c	U_{eq}
Ni	0.8362(1)	0.1381(1)	0.8077(2)	33(1)
N(1)	0.7800(8)	0.1027(10)	0.5736(16)	58(4)
N(2)	0.7399(7)	0.0502(9)	0.4862(13)	45(3)
N(3)	0.7992(8)	-0.0005(9)	0.8959(16)	57(3)
N(4)	0.9465(6)	0.0603(8)	0.7277(15)	46(3)
N(5)	0.8820(6)	0.2625(7)	0.6810(14)	39(2)
N(6)	0.7165(6)	0.2008(9)	0.8767(13)	44(3)
N(7)	0.8901(7)	0.1732(9)	1.0339(12)	45(3)
C(1)	1.0300(9)	0.1070(12)	0.7263(18)	60(4)
C(2)	1.0310(8)	0.1997(11)	0.6284(18)	52(4)
C(3)	0.9760(8)	0.2831(10)	0.6953(17)	46(3)
C(4)	0.8327(10)	0.3555(10)	0.7084(19)	58(3)
C(5)	0.7437(9)	0.3400(9)	0.6778(20)	52(4)
C(6)	0.6965(11)	0.3054(13)	0.8303(22)	72(5)
C(7)	0.6930(8)	0.1813(11)	1.0483(14)	43(3)
C(8)	0.7558(9)	0.2195(12)	1.1706(17)	51(4)
C(9)	0.8394(8)	0.1609(10)	1.1860(14)	49(3)
P	0.0204(3)	-0.0623(3)	0.2626(5)	48(1)
F(1)	0.0732(14)	-0.1433(19)	0.1678(27)	89(7)
F(2)	0.0339(17)	0.0086(19)	0.1072(29)	100(8)
F(3)	0.0008(17)	-0.1400(23)	0.4123(32)	108(8)
F(4)	-0.0338(25)	0.0160(32)	0.3553(47)	151(13)
F(5)	0.0981(18)	-0.0328(23)	0.3714(35)	123(11)
F(6)	-0.0616(19)	-0.0984(23)	0.1488(37)	118(10)
F(1)′	0.0354(15)	0.0474(17)	0.2981(31)	91(8)
F(2)′	0.1072(19)	-0.0797(22)	0.1881(41)	114(9)
F(3)′	-0.0674(13)	-0.0406(17)	0.3414(27)	74(7)
F(4)′	0.0540(19)	-0.0906(22)	0.4315(34)	103(9)
F(5)′	-0.0230(21)	-0.0337(25)	0.1004(37)	117(10)
F(6)′	-0.0065(19)	-0.1691(20)	0.2453(37)	115(11)

Results and Discussion

IR Spectra. ν_{as} of the azide groups appears at 2058 and 2104 (sh) cm^{-1} for **1** and 2127 and 2088 cm^{-1} for **2**. The N–H stretching of the 333-tet ligand appears at 3336, 3281, and 1606 cm^{-1} for **1** and 3355, 3300, and 1594 cm^{-1} for **2**. Bands attributable to the perchlorate and hexafluorophosphate appear at normal frequencies.

Description of the Structures. ***trans*-$[Ni(333\text{-tet})(\mu\text{-}N_3)]_n(ClO_4)_n$ (1).** The structure consists of 1D nickel–azido chains, isolated by ClO_4^- anions, which are found in the interchain space as shown in Figure 1. No hydrogen bonds between the chains or perchlorate groups are present. The most interesting feature of this compound is the existence of inversion centers at the central nitrogen of the azido groups; this produces a structurally alternating chain. A labeled scheme is shown in Figure 2A. The main bond lengths and angles are gathered in Table 4. In the chain structure, each Ni(II) atom is coordinated by one 333-tet ligand and two azido ligands in a distorted octahedral *trans* arrangement. The four N atoms of 333-tet ligand and the nickel(II) atom are in the same plane (maximum deviation from the plane for nitrogen is 0.047 Å for N(4); the nickel(II) ion is displaced by 0.112 Å). The two Ni–N(1) and Ni–N(4) distances are similar (2.117(3) and 2.121(3) Å) and shorter than the two Ni–N(2) and Ni–N(3) distances (2.152(3) and 2.150(3) Å, respectively). The two Ni–N bond distances to the nitrogen atoms of the azido bridge are quite different, being 2.077(3) Å for Ni–N(5) and 2.204(3) Å for Ni–N(7). The two bond angles related to the azido ligands are Ni–N(5)–N(6) (142.4(3)°) and Ni–N(7)–N(8) (123.6(2)°), the larger angle corresponding to the shorter bond distance. This feature is shown in Figure 3A. Each

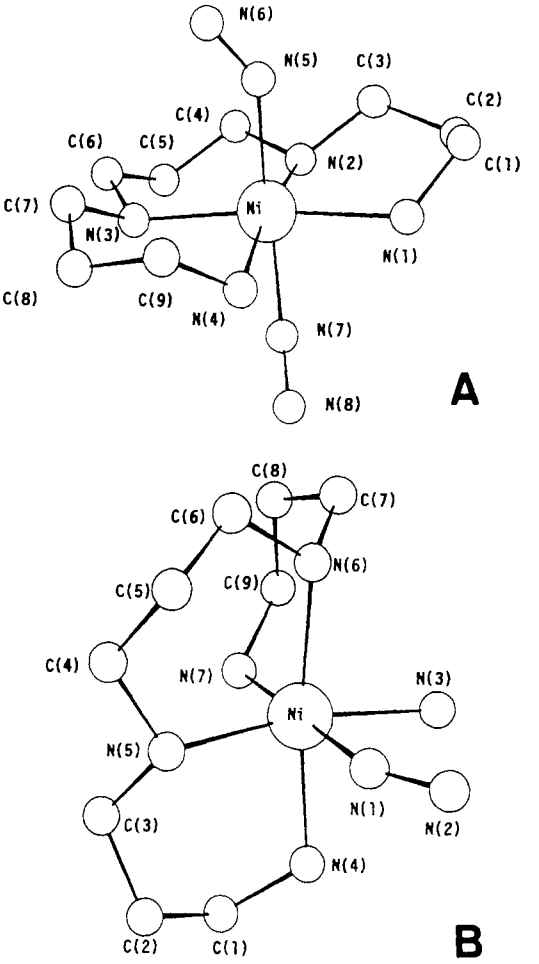

Figure 2. (A) Atom-labeled scheme of *trans*-$[Ni(333\text{-tet})(\mu\text{-}N_3)]_n(ClO_4)_n$ (**1**). (B) Atom labeled scheme for *cis*-$[Ni(333\text{-tet})(\mu\text{-}N_3)]_n(PF_6)_n$ (**2**).

Table 4. Selected Bond Distances (Å) and Angles (deg) for *trans*-$[Ni(333\text{-tet})(\mu\text{-}N_3)]_n(ClO_4)_n$ (**1**)

	Distances		
N(1)–Ni	2.117(3)	N(2)–Ni	2.152(3)
N(3)–Ni	2.150(3)	N(4)–Ni	2.121(3)
N(5)–Ni	2.077(3)	N(7)–Ni	2.204(3)
N(5)–N(6)	1.143(3)	N(8)–N(7)	1.155(3)
Ni–Ni′	6.003(1)	Ni′–Ni″	6.128(1)
	Angles		
N(2)–Ni–N(1)	89.2(1)	N(3)–Ni–N(1)	172.3(1)
N(3)–Ni–N(2)	97.1(1)	N(4)–Ni–N(1)	86.6(1)
N(4)–Ni–N(2)	170.8(1)	N(4)–Ni–N(3)	86.5(1)
N(5)–Ni–N(1)	89.9(1)	N(5)–Ni–N(2)	92.8(2)
N(5)–Ni–N(3)	94.2(1)	N(5)–Ni–N(4)	95.4(2)
N(7)–Ni–N(1)	88.9(1)	N(7)–Ni–N(2)	81.3(1)
N(7)–Ni–N(3)	87.7(1)	N(7)–Ni–N(4)	90.4(1)
N(7)–Ni–N(5)	174.0(1)	N(6)–N(5)–Ni	142.4(3)
N(8)–N(7)–Ni	123.6(2)	N(5)–N(6)–N(5)′	180.0
N(7)–N(8)–N(7)′	180.0		

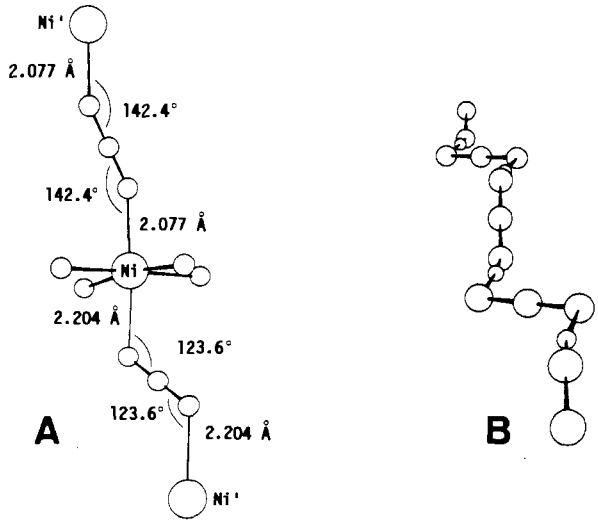

Figure 3. (A) Fragment of *trans*-$[Ni(333\text{-tet})(\mu\text{-}N_3)]_n(ClO_4)_n$, showing the bond angles and distances of two neighboring azido groups. Only the skeleton nickel(II)–nitrogen is shown for clarity. (B) Axial view of the same fragment of *trans*-$[Ni(333\text{-tet})(\mu\text{-}N_3)]_n(ClO_4)_n$, showing the torsion between neighboring azido groups. The nickel atoms are reduced in size for clarity.

Table 5. Selected Bond Distances (Å) and Angles (deg) for *cis*-$[Ni(333\text{-tet})(\mu\text{-}N_3)]_n(PF_6)_n$ (**2**)

	Distances		
N(1)–Ni	2.164(13)	N(3)–Ni	2.102(11)
N(4)–Ni	2.136(11)	N(5)–Ni	2.112(10)
N(6)–Ni	2.143(10)	N(7)–Ni	2.091(10)
N(2)–N(1)	1.19(2)	N(3)'–N(2)	1.17(2)
Ni–Ni'	6.182(6)		
	Angles		
N(3)–Ni–N(1)	89.5(5)	N(4)–Ni–N(1)	87.2(5)
N(4)–Ni–N(3)	83.4(5)	N(5)–Ni–N(1)	83.3(5)
N(5)–Ni–N(3)	169.3(5)	N(5)–Ni–N(4)	88.2(4)
N(6)–Ni–N(1)	87.8(5)	N(6)–Ni–N(3)	91.4(5)
N(6)–Ni–N(4)	172.8(4)	N(6)–Ni–N(5)	96.3(4)
N(7)–Ni–N(1)	179.6(5)	N(7)–Ni–N(3)	90.8(5)
N(7)–Ni–N(4)	93.2(4)	N(7)–Ni–N(5)	96.5(4)
N(7)–Ni–N(6)	91.9(4)	N(2)–N(1)–Ni	151.8(11)
N(2)'–N(3)–Ni	151.3(12)	N(1)–N(2)–N(3)'	177.9(14)

fragment of five Ni–N_3–Ni atoms is coplanar, and consequently the torsion angle is 0°. The torsion angle between neighboring azido groups is 93.4° as shown in Figure 3B. Due to the symmetric Ni–N–N bond angles and the Ni–N_3–Ni torsion angle, the neighboring nickel-N_4 amine planes are parallel.

The structure of *trans*-$[Ni(333\text{-tet})(\mu\text{-}N_3)]_n(ClO_4)_n$ shows three important features related with the azido bridging ligand which influence the overlap and consequently the magnetic results, as discussed below: (1) The five atoms of each Ni–NNN–Ni unit of the chain are placed in the same plane. (2) The N–N–Ni angles in each unit are of two different types with values of 142.4 and 123.6°. (3) The Ni–N distances are also different (2.077 and 2.204 Å), with the larger distances corresponding to the smaller angles.

***cis*-$[Ni(333\text{-tet})(\mu\text{-}N_3)]_n(PF_6)_n$ (2).** This structure consists also of a 1D nickel–azido system isolated by PF_6^- anions placed in the interchain space. The labeling scheme is shown in Figure 2B. The main bond lengths and angles are gathered in Table 5. Each nickel atom shows an octahedral environment with coordination to a 333-tet ligand in *cis* fashion and to two end-to-end azido bridges. The N(4), N(5), and N(6) atoms of 333-tet are placed in the same plane, but in contrast to **1**, N(7) is axial to this plane. The three Ni–N(4), Ni–N(5), and Ni–N(6) distances are similar (2.136(11), 2.112(10), and 2.143(10) Å, respectively) and longer than the fourth Ni–N(7) distance of 2.091(10) Å. The Ni–N(1) and Ni–N(3) distances are 2.164(13) and 2.102(11) Å, respectively. The most significant feature of this structure is the unusually large value of the nickel–azido bond angles: Ni–N(1)–N(2) = 151.8(11)° and Ni–N(3)–N(2)' = 151.3(12)°. The Ni–N(1)–N(3)–Ni' torsion angle is 37.2°, and the extension of this torsion to the 1D system leads to a helicoidal nickel–azido skeleton as is shown in Figure 4.

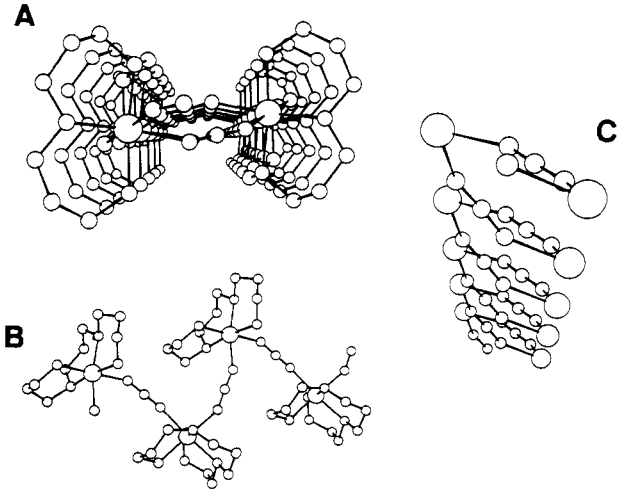

Figure 4. (A) Axial view of *cis*-$[Ni(333\text{-tet})(\mu\text{-}N_3)]_n(PF_6)_n$ (**2**). (B) Perpendicular view of **2**. (C) Helicoidal nickel–azido skeleton of **2**.

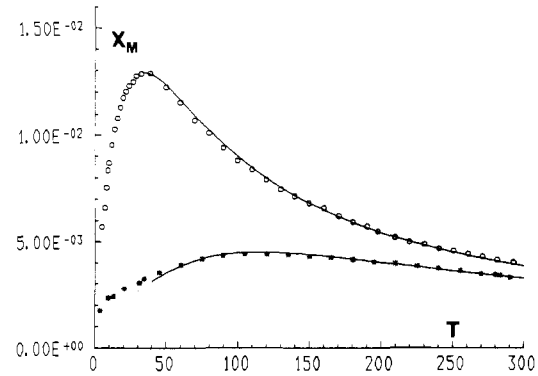

Figure 5. Magnetic susceptibility plots of a polycrystalline sample for *trans*-$[Ni(333\text{-tet})(\mu\text{-}N_3)]_n(ClO_4)_n$ (*) and *cis*-$[Ni(333\text{-tet})(\mu\text{-}N_3)]_n(PF_6)_n$ (o). Solid lines show the best fit obtained (see text).

The factors that can be related to the magnetic behavior are in this case (1) the high value of the Ni–N_3–Ni torsion angle (37.2°) and (2) the very high value of both Ni–N–N angles, ≈150°.

Magnetic Results. The molar magnetic susceptibilities *vs T* of *trans*-$[Ni(333\text{-tet})(\mu\text{-}N_3)]_n(ClO_4)_n$ (**1**) and *cis*-$[Ni(333\text{-tet})(\mu\text{-}N_3)]_n(PF_6)_n$ (**2**) are plotted in Figure 5. The χ_M values (3.31×10^{-3} for **1** and 4.01×10^{-3} $cm^3 \cdot mol^{-1}$ for **2** at room temperature) increase when temperature decreases, reaching a broad maximum *ca.* 115 K for **1** and a well-defined maximum *ca.* 39 K for **2**, with χ_M values of 4.40×10^{-3} and 1.29×10^{-2} $cm^3 \cdot mol^{-1}$, respectively. Below these temperatures, the curves decrease continuously and reaches the values of 1.75×10^{-3} for **1** and 5.71×10^{-3} $cm^3 \cdot mol^{-1}$ for **2** at 4 K. The plot of **1** agrees with the theoretical behavior for an alternating system, whereas the one for **2** should be indicative of a Haldane effect. The position of the maxima clearly indicates strong antiferromagnetic coupling between nickel(II) ions through the azido bridge for **1** and lower antiferromagnetic coupling for **2**.

In a first approach, experimental data have been fitted to the Weng equation,[30] based upon the spin Hamiltonian $H = -J\Sigma S_i S_{i+1}$, where the nickel ion is assumed to be magnetically isotropic:

(30) Weng, C. Y. Ph.D. *Thesis*, Carnegie Institute of Technology, 1968.

$$\chi_M = (N\beta^2g^2/kT)(2 + A\delta + B\delta^2)/(3 + C\delta + D\delta^2 + E\delta^3)$$

in which $A = 0.019$, $B = 0.777$, $C = 4.346$, $D = 3.232$, $E = 5.834$, and $\delta = |J|/kT$. A good fit is only possible down to temperatures near the maximum in χ (in our case up to 100 K for **1** and 30 K for **2**), because neither zero-field splitting nor the Haldane gap effect is taken into account in the equation. The J value has been obtained by minimizing the function $R = \Sigma(\chi_M^{calcd} - \chi_M^{obs})^2/\Sigma(\chi_M^{obs})^2$. The best fitting parameters obtained are $J = -62.1$ cm^{-1}, $g = 2.45$, $R = 9.01 \times 10^{-4}$ for **1** and $J = -18.5$ cm^{-1}, $g = 2.29$, and $R = 1.41 \times 10^{-4}$ for **2**. An equation for the analysis of magnetic susceptibility data of alternating chains with local $S = 1$ has been recently proposed by Borras,[31] for calculations on a cyclic system of four spin pairs that gives a good approximation up to $kT/J_1 = 0.4$. By using this expression, the value of the coupling parameters for **1** has been optimized up to the values $J = -80.7$ cm^{-1}, $J' = -37.4$ cm^{-1} ($\alpha = 0.46$), $g = 2.40$, and $R = 9.5 \times 10^{-5}$. It is interesting to point out that the value of J obtained by using the Weng equation is very close to the mean of the calculated values for an alternating system.

MO Calculations. The most suitable method for the treatment of the superexchange interaction through an azido bridge has been controversial in recent years. The first approach was made by means of MO extended-Hückel calculations,[2] but more recently Kahn and co-workers[4] have noted that the spin polarization model describes the superexchange for the azido ligand more correctly, particularly for the EO coordination, where the accidental orthogonality of the magnetic orbitals appears to be especially unsatisfactory. Subsequent studies on coupled dimers[14,15,32] and chains[21] for EE azido bridges seem to indicate that, at least for this coordination mode, MO extended-Hückel calculations are appropriate, and we will use this model to correlate the magnetic properties in our compounds.

MO extended-Hückel calculations have been performed by means of the CACAO program,[33] on a dimeric fragment which can be assumed as the translational unit that generates the 1D system:

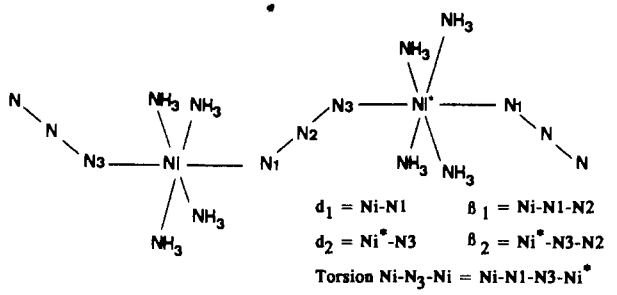

The general calculations were performed by varying the β_1, β_2, and Ni–N_3–Ni angles and maintaining $d_1 = d_2 = Ni–NH_3 = 2.10$ Å and N1–N2 = N2–N3 = 1.17 Å. For the particular cases, d_1 and d_2 distances and the β_1, β_2, and Ni–N_3–Ni angles were those summarized in Table 6. Atomic parameters used were the standards of the program. The same scheme and bond parameters, extended to three nickel centers, were used in the calculations involving three nickel units in *cis* or *trans* arrangements.

For a [NiNi] system, the antiferromagnetic component of J is a function[34] of $D^2(xy) = |E\Phi(xy_{(s)}) - E\Phi(xy_{(a)})|^2$ and $D^2(z^2) = |E\Phi(z^2_{(s)}) - \Phi(z^2_{(a)})|^2$. For a *trans* chain in which the d(z^2) orbitals are placed in the chain direction, only the z direction is operative as an exchange pathway, $D^2(xy)$ value is zero, and J_{AF} is only a function of $D^2(z^2)$. A set of 19 × 19 $D^2(z^2)$ values were calculated in 5° intervals for β_1 and β_2 between 90 and 180°, maintaining the torsion angle Ni–N_3–Ni = 0°; the results are shown in Figure 6A. From this figure, the maximum coupling is expected for $\beta_1 = \beta_2 = 108°$ and for greater β values the antiferromagnetic interaction must decrease. An accidentally orthogonal valley, centered on $\beta_1 = \beta_2 = 164°$, between the two σ and π exchange pathways previously described,[21] is found. This plot agrees with the generally accepted assumption that the main interaction is through the π pathway using the nonbonding MO of the azido ligand and the σ pathway is poorly operative. Our results indicate that this superexchange pathway is strongly dependent on the β_1 and β_2 bond angles.

The effect of the Ni–N_3–Ni torsion angle has been parametrized by means of a set of 19 × 11 values of $D^2(z^2)$ for a symmetric variation of $\beta_1 = \beta_2$ between 90 and 180° and Ni–N_3–Ni torsion angles every 5° between 0 and 50°. The result is shown in Figure 6B. For all β values, the maximum coupling can be expected for a torsion value of zero, decreasing gradually when the torsion angle increases. The magnitude of this effect is lower than the effect of the bond angle and can be considered as a secondary term that tunes the main factor. As an example, 30° of variation in β between 120 and 150° reduces the D^2 value by *ca.* 91%, whereas, for both angles, 30° of variation in the Ni–N_3–Ni torsion angle reduces the D^2 value by *ca.* 30%.

Finally, calculations varying d_1 and d_2 in the range 2.05–2.20 Å and maintaining constant values for $\beta_{1,2}$ and the Ni–N_3–Ni torsion angle indicate that lower values of $D^2(z^2)$ occur for the larger $d_{1,2}$ distances, and their magnitude is of the same order as that produced by the variation of the Ni–N_3–Ni torsion angle. As an example, a variation of $d_{1,2}$ between 2.09 and 2.21 Å reduces the D^2 value by *ca.* 35%.

On the other hand, calculations involving three nickel atoms and placing the azido bridges in *trans* or *cis* arrangement show the same general behavior for ΣD^2 (in a *cis* conformation $D^2(xy)$ is not zero), indicating, as expected, that the main factors are the bond parameters involving each bridge and not how this unit is repeated along one axis.

Summarizing the above results, it can be concluded that in a correlation between the magnetic behavior and structural parameters for monobridged azido chains, the bond parameters that must be taken into account are (in this order) the bond angles $\beta_{1,2}$, the torsion angle Ni–N_3–Ni, and finally the bond distances $d_{1,2}$.

In order to check this model with the experimental facts, Table 6 shows the $\Sigma D^2(xy,z^2)$ values obtained using the real bond parameters for a series of 1D monobridged nickel(II)–azido compounds. According to the above conclusions, for the alternating chain **1** two very different values of J are expected for the two different bridges, and effectively, experimental values of –80.7

Table 6. Main Structural and Magnetic Parameters for (μ-N_3)[NiL]$^+$ Monobridged Systems[a]

	compound[b]						
	1	1′	2	3	4	5	6
d_1, Å	2.204	2.077	2.102	2.150	2.165	2.156	2.129
d_2, Å	2.204	2.077	2.164	2.150	2.172	2.151	2.181
β_1, deg	123.6	142.4	151.3	142.0	140.7	134.6	135.8
β_2, deg	123.6	142.4	151.8	142.0	128.2	124.1	119.8
Ni–N_3–Ni, deg	0.0	0.0	37.2	0.0	13.1	37.6	10.7
$D^2(z^2)$	0.219	0.113	0.005	0.085	0.133	0.130	0.207
J, cm^{-1}	–80.7	–37.4	–18.5	–24.4	–39.2	–26.9	–62.7
ref	*c*	*c*	*c*	6, 7	20	21	21

[a] The D^2 values correspond to those found by using the structural parameters reflected in this table. It must be pointed out that the complex with tmcyclam is not a 1D system but a dinuclear one with the same pattern as for the four 1D chains. [b] 1 and 2, L = 333-tet; 3, L = tmyclam, 1,4,8,11-tetramethyl-1,4,8,11-tetraazacyclotetradecane; 4, L = cyclam; 5, L = 232-tet, *N*,*N*′-bis(2-aminoethyl)-1,3-propanediamine; 6, L = 323-tet, *N*,*N*′-bis(3-aminopropyl)-1,2-ethanediamine. [c] This work.

(31) Borras, J. J. Ph.D. *Thesis*, Universitat de Valèncía, Spain, 1991.
(32) Kahn, O.; Mallah, T.; Gouteron, J.; Jeannin, S.; Jeannin, Y. *J. Chem. Soc., Dalton Trans.* **1989**, 1117.
(33) Mealli, C.; Proserpio, D. M. CACAO program (Computed Aided Composition of Atomic Orbitals). *J. Chem. Educ.* **1990**, *67*, 399.
(34) Hay, P. J.; Thibeault, J. C.; Hoffmann, R. *J. Am. Chem. Soc.* **1975**, *97*, 4884.

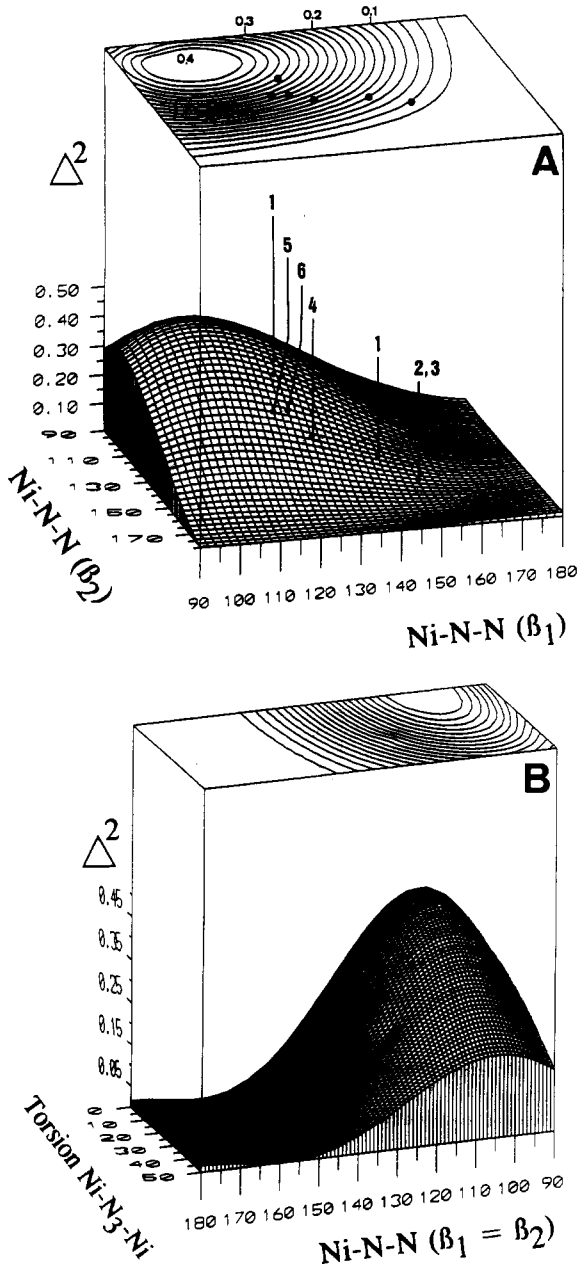

Figure 6. (A) Plot of D^2 in function of β_1 and β_2 for a [NiNi] monobridged EE azido system. The sets of the experimentally β values for *catena*-(μ-N_3)[NiL]X systems are referenced in Table 6. (B) Plot of D^2 as a function of the torsion angle and with the assumption $\beta_1 = \beta_2$.

cm^{-1} (assigned to the bridge in which $\beta_1 = \beta_2 = 123.6°$) and -37.4 cm^{-1} (assigned to the bridge in which $\beta_1 = \beta_2 = 142.4°$) have been found. The alternating parameter α is 0.46 and the theoretical ratio between the calculated gaps is 0.52, showing an excellent agreement with the experimental value. According to the structural data, the -80.7-cm^{-1} J value is the highest found for a single azido bridge and it correlates with the β angle of 123.6°, which is the lowest Ni–N–N angle reported to date. For the *cis* compound **2**, a low $-J$ value is expected because of the high values of both β (maximum Ni–N–N angle reported to date) and torsion angles; this is in good agreement with the experimental value of -18.5 cm^{-1}, which is the lowest $|J|$ value found for a single azido bridge. The agreement between the values of D^2 *vs* $|J|$ reported in Table 6, for all the nickel(II)–azido monobridged systems reported in the literature, is presumably a good indication of the validity of this model.

Finally, this model can be related to the recent work[14] of Ribas *et al.* in which the superexchange parameter J has been correlated as function of the angle Γ for dinuclear di-μ-azido systems.

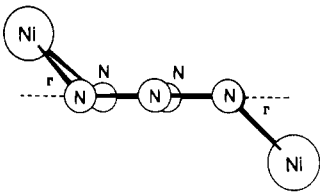

For a dinuclear system, in which the two azido ligands are experimentally always parallel, if the angle $\Gamma = 0$ and the angles N–Ni–N $\approx 90°$, the four Ni–N–N angles must take values centered around 135°, and any increase of two of these angles must be compensated for a decrease in the other two.

According to our model, for a system in which Ni–N–N = 135° and the Ni–N_3–Ni torsion angle is 180 or 0°, the D^2 parameter takes a value of 0.18; this can be translated to an estimate J value of ≈ -50 cm^{-1} for each azido bridge by extrapolation of the experimental results showed in Table 6 for monobridged systems. Two compounds[8,14] with two azido bridges and an arrangement nearly planar ($\Gamma = 3.0$ and 6.8°) have been reported, and effectively, the corresponding J values are -114.5 and -90 cm^{-1}. This correlation is only a qualitative approach, but the possibility of linking our correlations with the work on dinuclear systems of ref 14 shows the coherence of our proposition with all the magnetic results reported to date for the nickel–azido bridged systems.

Concluding Remarks

In this work, two novel kinds of monobridged nickel(II)–azido systems are obtained and a general and simple model to correlate magnetic and structural parameters for this coordination mode of the azido ligand has been proposed. This model rationalizes the magnetic behavior in a different way from the effect of spin polarization proposed by Kahn,[4] but the two methods give the same general conclusions, and we think that in spite of the good results of our model, a definitive explanation of the magnetic properties of this ligand is still necessary.

Acknowledgment. This work was undertaken with the financial support of the CICYT through Project PB91/0241.

Supplementary Material Available: Tables giving crystal data and details of the structure determination, bond lengths, bond angles, anisotropic thermal parameters, and hydrogen atom locations and ORTEP diagrams (16 pages). Ordering information is given on any current masthead page.